Hindawi
Advances in Civil Engineering
Volume 2018, Article ID 2318063, 10 pages
https://doi.org/10.1155/2018/2318063

Research Article

Numerical Tests Research on Mechanical Parameters of Rockmass considering Structural Plane Combination Characteristics

Jihong Wei,[1] **Yan Men**,[1] **Shaorui Sun**,[1] **Yajie Wang**,[2] **Wei Qian**,[1] **and Wei Shi**[1]

[1]*School of Earth Science and Engineering, Hohai University, Nanjing 210098, China*
[2]*Shanghai Tunnel Engineering Co. Ltd., Shanghai 200082, China*

Correspondence should be addressed to Shaorui Sun; sunsrhhu@163.com

Received 3 May 2018; Revised 22 July 2018; Accepted 1 August 2018; Published 27 August 2018

Academic Editor: Xiang Fan

It is essential to determine rockmass mechanical parameters in stability assessment. The structural z is the main factor in this regard, and we know little about the relationship between mechanical parameters and multiple structure planes. In this paper, we have conducted a series of numerical tests to obtain mechanical parameters for a dam foundation in Southwest China. The biaxial numerical test was performed based on the discrete element method. This numerical test considers the spacing, types, dip angles, and size effect. We established a relationship of mechanical parameters between small size lab samples and large size field samples. We forecasted the strength parameters for a spillway slope in Southwest China. The dip angle has a significant effect on the slope strength and stability. In this case, the rockmass fracture stress-dip angle curve forms a U-shaped distribution. The X-shaped double structure plane demonstrates severe strength weakening relative to a single structure plane. As structure plane spacing reaches a certain level, its influence on rockmass strength diminishes. The elementary volume of the rockmass for dam foundation analysis is about $4\,\text{m} \times 4\,\text{m} \times 4\,\text{m}$.

1. Introduction

Conventional rock mechanical tests consider an intact rock, and the influence of multiple structure planes is ignored [1–5]. Rockmass is a multibody system with many structure planes and it is well known that many accidents of rock failure is due to the lack of research on structure planes. From the 1960s to the late 1980s, a pioneer geological engineer [6] proposed the rockmass structure control theory to conduct systematic and comprehensive studies in this regard. Many other researchers have also achieved a significant number of results [7–11]. The most common methods used today for mechanical parameters assessment are engineering analogy, lab and field tests, numerical simulation, and counter-analysis [12–18]. Numerical simulation is the most efficient due to the fact that the characteristics of the structure planes can be taken into account [19–22]. From the perspective of homogenization, people have studied the rockmass mechanical parameters [23–26]. From the basic concept of representative elementary volume (REV), the mechanical significance of REV model is derived. The determination method for jointed rockmass strength is also developed. Research regarding jointed rockmass mechanical properties remains an interesting topic. In this paper, we present a numerical test case for a spillway slope, located at the Jinsha River in Southwest China. We have designed jointed rockmass analogy simulation with a focus on the influence of structure plane characteristics.

2. Procedures of Numerical Test

The influence mechanism of dip angles and structure plane densities on its rockmass mechanical parameters are studied through rockmass numerical tests of the structure plane (Figures 1 and 2). Due to the fact that the structure plane involves a large number of geometric characteristics, it is not possible to conduct an accurate simulation. In order to facilitate the study of the influence of dip angle, number,

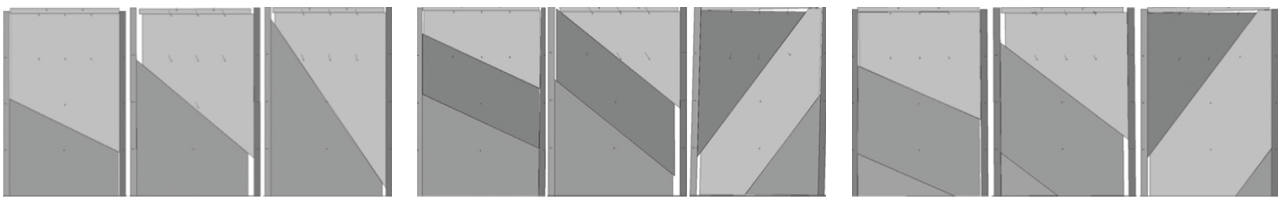

(a) (b) (c)

Figure 1: Failure maps of samples under numerical simulation. (a) Different dip angles. (b) Spacing with 30 mm. (c) Spacing with 45 mm.

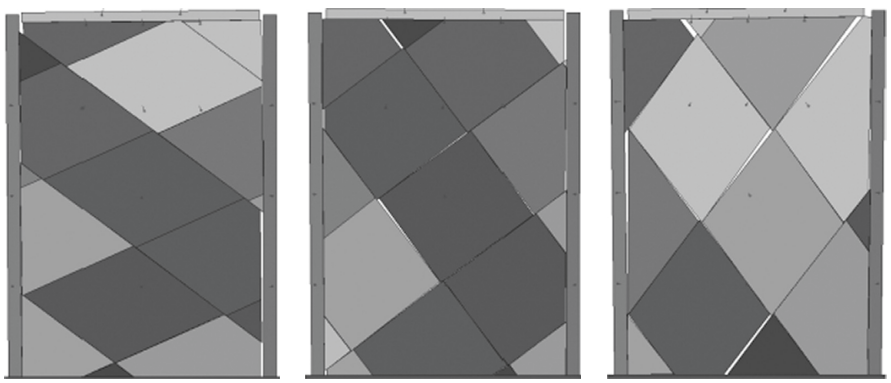

(a) (b) (c)

Figure 2: Rock failure maps under different combination of dip angles. (a) 30°–45°. (b) 45°–60°. (c) 60°–60°.

density, and other factors on the rockmass mechanical parameters of structure plane, the rockmass joints are abstracted and generalized into ideal model samples, and the model is simplified using the following assumptions: (1) the structure plane of the rockmass sample is a flat surface, i.e., do not consider the influence of rough patches on the structure plane on the experimental results, instead only consider the dip angle, number, and bond strength of the structure plane; and (2) Ignore the influence of tiny fissures on the experimental results.

Seven groups of single-jointed rock mass samples were prepared with varying structural plane angles of 0°, 15°, 30°, 45°, 60°, 75°, and 90°. Three groups of X-shaped combination structural surfaces were prepared for rockmasses containing the plane angle combinations of 30–45, 45–60, and 60–60 and having spacing of 10, 30, 60, and 100 cm for single joint and 10, 50, and 100 cm for X-shaped joint, respectively, were prepared. Three samples in each group were tested to obtain the average value. Tests were conducted under the confining pressures of 1.5, 2.5, 3.5, and 6.0 MPa, until the samples were damaged.

3. Influence of Structure Planes Characteristics on Rockmass Mechanical Parameters

3.1. Dip Angle. A numerical model (Figure 1) was created and then the different confining pressures, such as 1.5, 2.5, 3.5, and 6.0 MPa, were selected for performing numerical analysis according to the laboratory test values. The dip angle ranged from 0 to 90°, and the value at each interval of 15° was read (for a total of seven values, i.e. 0°, 15°, 30°, 45°, 60°, 75°, and 90°). Based on the above numerical simulation, data was obtained, and are given in Table 1.

According to the loading conditions in the laboratory, the confining pressures were set to 1.5, 2.5, 3.5, and 6.0 MPa, and the dip angles ranged from 0 to 90°, with a spacing of 15°. It can be seen from Figure 3 that the fracture stress increases with the increase in confining pressure. The fracture stress curve shows an approximate U-shaped distribution with the dip angle being changed. When the dip angle is either 0 or 90°, the fracture stress value is greater and close to the rock fracture strength, which also shows that at this time the rock strength controls the rockmass fracture strength. The fracture stress attains its minimum value when the dip angle is 60°. This fracture stress and the compressive strength of rock are greatly different, which shows that at this time the structure plane controls the rockmass fracture.

After comparing the laboratory and numerical simulation results, which are shown in Figure 3, it can be seen that the results of the numerical simulation and laboratory tests [27] show a high level of consistency. The laboratory results show that the fracture curve forms an approximate U-shaped distribution with the dip angle being changed, and the rockmass strength reaches its minimum value when the dip angle is 60°. The experimental results are not regular, which is due to the influence of many factors occurring in laboratory tests. Certain degrees of errors in numerical simulation and laboratory data are permitted, provided that the influence of controlling factors in the system may be reflected, and that the errors are within a certain range.

Table 1: Fracture stress values of rockmass with structure planes of different dip angles.

Confining pressure (MPa)	Fracture stress values (MPa)						
	0°	15°	30°	45°	60°	75°	90°
1.5	32.0	30.7	28.4	6.57	6.0	21.6	31.4
2.5	40.7	39.3	36.5	10.4	9.4	29.7	40.4
3.5	49.4	47.8	44.5	14.3	12.7	36.7	50.5
6.0	71.7	69.6	65.1	24.1	22.3	53.0	74.7
Cohesion (MPa)	3.14	3.01	2.82	0.17	0.09	2.28	2.67
Internal friction angle (°)	52.80	52.43	51.41	36.29	34.64	48.33	54.35

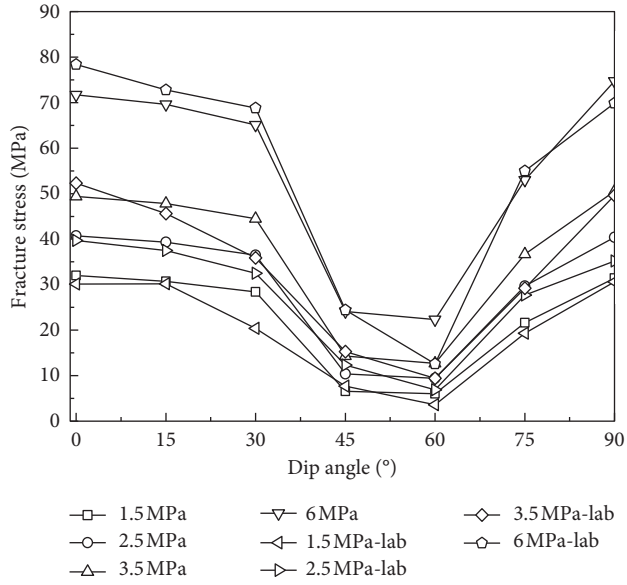

Figure 3: Numerical simulation and analogy experimental results of fracture stress of rockmass with different dip angles.

Therefore, it is credible to simulate the rockmass containing structure planes with analogy materials, which may aid in revealing some of the influence mechanisms.

3.2. Number of Structure Plane. Based on the simulation of rockmass fractures with a group of structural surfaces, two groups of rockmass structural surfaces are considered. The purpose of the numerical simulation is to study the rockmass mechanical parameters of two groups of structure planes at different dip angles. The numerical model is built on the basis of the X-shaped intersected engineering jointed rockmass. In order to facilitate analysis, several groups of typical combined dip angles are selected for analysis. The dip angles of 0° and 90° have little effect on the jointed rockmass, and those of 15° and 75° have even less effect. Therefore, the combinations intersected by structure planes with angles of −30°, −45°, and −60° and structure planes with the seven different angles of 0°, 15°, 30°, 45°, 60°, 75°, and 90° are selected. The confining pressure values are still kept as 1.5, 2.5, and 3.5 MPa. After observing the results of the above numerical test, the experimental data are listed in Table 2.

Through comparison of the axial fracture stress simulation values (Figure 4 and Table 2) and measured values (Figure 3 and Table 1) of combined X-shaped jointed rockmass with dip angles of 30, 45, and 60° under different confining pressures, it may be seen that a small deviation exists between the local data of the laboratory test values and the numerically simulated values, and the conformity of the overall trend is quite high. On one hand, it is sufficient to prove the feasibility of analogy simulation tests, and on the other, the results also show that the calculation parameters selected for the numerical simulation are reasonable. Thus it may be concluded that it is a feasible and effective means to study the reasonable selection of rockmass parameters and the influence patterns of all factors on rockmass parameters through the combined application of numerical simulation and analogy tests.

It can be seen from Figure 5(a) that the fracture stress trend of a rockmass with a combined structure plane of −30° is almost identical to that of a rockmass with a single structure plane. The fracture stress value decreases significantly under the same confining pressure. As shown in Figures 5(b) and 5(c), the fracture stresses of rockmass with a combined structure plane of −45° and −60° are arranged in parallel straight lines. The fracture stresses of rockmass with combined structure planes are basically identical to those of a single structure plane under a certain confining pressure. These results indicate that the structure plane with the dip angle being 45° to 60° plays a controlling role in the rockmass with a combined structure plane being 45° and 60°. The strength of the structure planes with any other angles or those combined by these angles is reduced to the level of the controlling structure plane, due to the existence of the controlling structure plane. Therefore, the controlling structure plane plays a decisive role in the strength of the rockmass.

According to the results of these numerical simulations, the comprehensive cohesive strength and internal friction angle curves of rockmass with different dip angles are shown in Figure 6. As seen in Figure 6(b), the internal friction angles of rockmass with a combined structure plane being −30°, −45°, and −60° decrease with the increase of dip angle in the same combination, and those with a combined structure plane being −30° form a funnel shape with the changes in the dip angle. The curve of the combined structure plane being −45° and −60° is almost a horizontal straight line, which also shows that 45° to 60° is the controlling dip angle of the rockmass. Compared with a single structure plane with a different dip angle, the structure plane being −45° to −60° shows clear parameter weakening effects on the rockmass, which is the most adverse structure plane. The cohesive strength of rockmass with structure planes of different dip angles is shown in Figure 6(a). As seen, the cohesive strength of the −30° combination is significantly higher than that of the combination of −45° and −60°. The comprehensive cohesive strength value of the −60° combination is slightly greater than that of the −45° combination. However, the comprehensive internal friction angle of the −60° combined dip angle is smaller than that of −45° (Figure 6(b)). The cohesive strength of rockmass with a −45°

Table 2: Numerical simulation results of fracture stress values of rockmass with different structure plane combinations.

Confining pressure (MPa)	0°	15°	30°	45°	60°	75°	90°
Fracture stress values under the condition of combination structural surface −30° (MPa)							
1.5	25.30	23.80	23.10	6.78	6.71	18.40	28.40
2.5	33.00	30.40	29.80	10.70	10.40	24.80	36.80
3.5	40.10	37.10	36.60	14.60	14.20	30.90	44.90
Cohesion (MPa)	2.63	2.68	2.49	0.23	0.28	1.82	2.80
Internal friction angle (°)	49.63	47.61	47.90	36.25	35.35	46.40	51.61
Fracture stress values under the condition of combination structural surface −45° (MPa)							
1.5	6.73	6.67	6.55	6.70	6.69	6.79	6.62
2.5	10.60	10.50	10.40	10.50	10.60	10.60	10.50
3.5	14.50	14.40	14.30	14.50	14.20	14.50	14.40
Cohesion (MPa)	0.23	0.22	0.19	0.21	0.29	0.25	0.20
Internal friction angle (°)	36.20	36.08	36.14	36.29	35.41	36.02	36.23
Fracture stress values under the condition of combination structural surface −60° (MPa)							
1.5	6.50	6.69	7.47	6.89	6.60	7.00	6.01
2.5	9.96	10.20	11.20	10.50	10.50	10.90	9.40
3.5	13.60	13.90	14.80	14.10	13.90	14.80	12.80
Cohesion (MPa)	0.30	0.33	0.52	0.39	0.32	0.29	0.25
Internal friction angle (°)	34.09	34.45	34.84	34.45	34.74	36.29	33.02

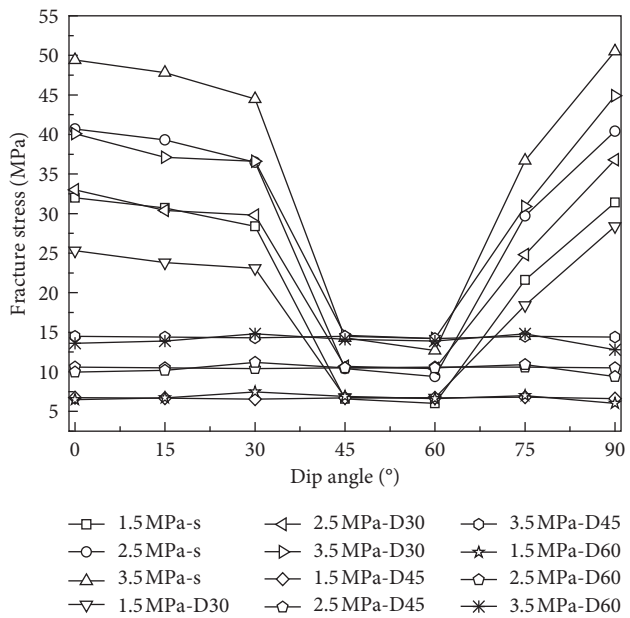

Figure 4: Fracture stress values of X-shaped structure plane rockmass under the dip angle with different combination (*s* represents single structure plane, and *D* represents double structure plane).

combined structural surface is relatively close to that of −60°. The influence of the 45° to 60° structure plane on the rockmass parameters is as decisive as the controlling structure plane. In addition, the double-jointed rockmass has clear weakening effects on the parameters of single-jointed rockmass.

3.3. The Spacing of Structure Plane. The rockmass contain microcracks, joints, and other structure planes, which is a great difference with the respective mechanical parameters of rock blocks.

As shown in Figure 7, the number of structure planes increase with the volume. Furthermore, the rockmass strength significantly varies from intact rock block to jointed rockmass. The mechanical properties of rockmass with smaller scale are instability. The noncontinuous medium of the rockmass with greater scale can be deemed as an equivalent continuous medium. The representative elementary volume (REV) of the rockmass is presented in Figure 8. REV contains the oppositions and unifications of "micro and macro," "discreteness and continuity," and "randomness and consistency." Based on the micro method, all materials are noncontinuous and contain randomly distributed discontinuities. Their mechanical properties are bound to show a random wave with space and volume. However, with the macro method, when these REV values reach a greater scale, they can be considered as the equivalent continuous media and their macro mechanical properties will become stable.

The influence of macro weak structure planes on the mechanical parameters of rockmass are studied in this paper. The completely interconnected structure planes are first observed to simplify the analysis model. The influence of rock bridge and jointed trace are not considered to the influence of spacing between different rockmass structure planes on its mechanical parameters.

In order to identify the REV rockmass size with structural surface, first, the rockmass mechanical parameters were obtained. Then, based on the results of laboratory tests, triaxial numerical simulations of mechanical parameter of rockmasses with different joint spacings and sizes were conducted. Triaxial tests of rockmass with side lengths of 0.5, 1.0, 2.0, 3.0, 4.0, 5.0, and 6.0 m were simulated by using discrete element numerical values under the confining pressure of 1.5 MPa in numerical simulation tests. During these simulations, the joint spacings were set to 0.1, 0.3, 0.5, 0.6, and 1.0 m.

The fracture stresses of rockmass with different spacing in the numerical tests are shown in Table 3. The fracture

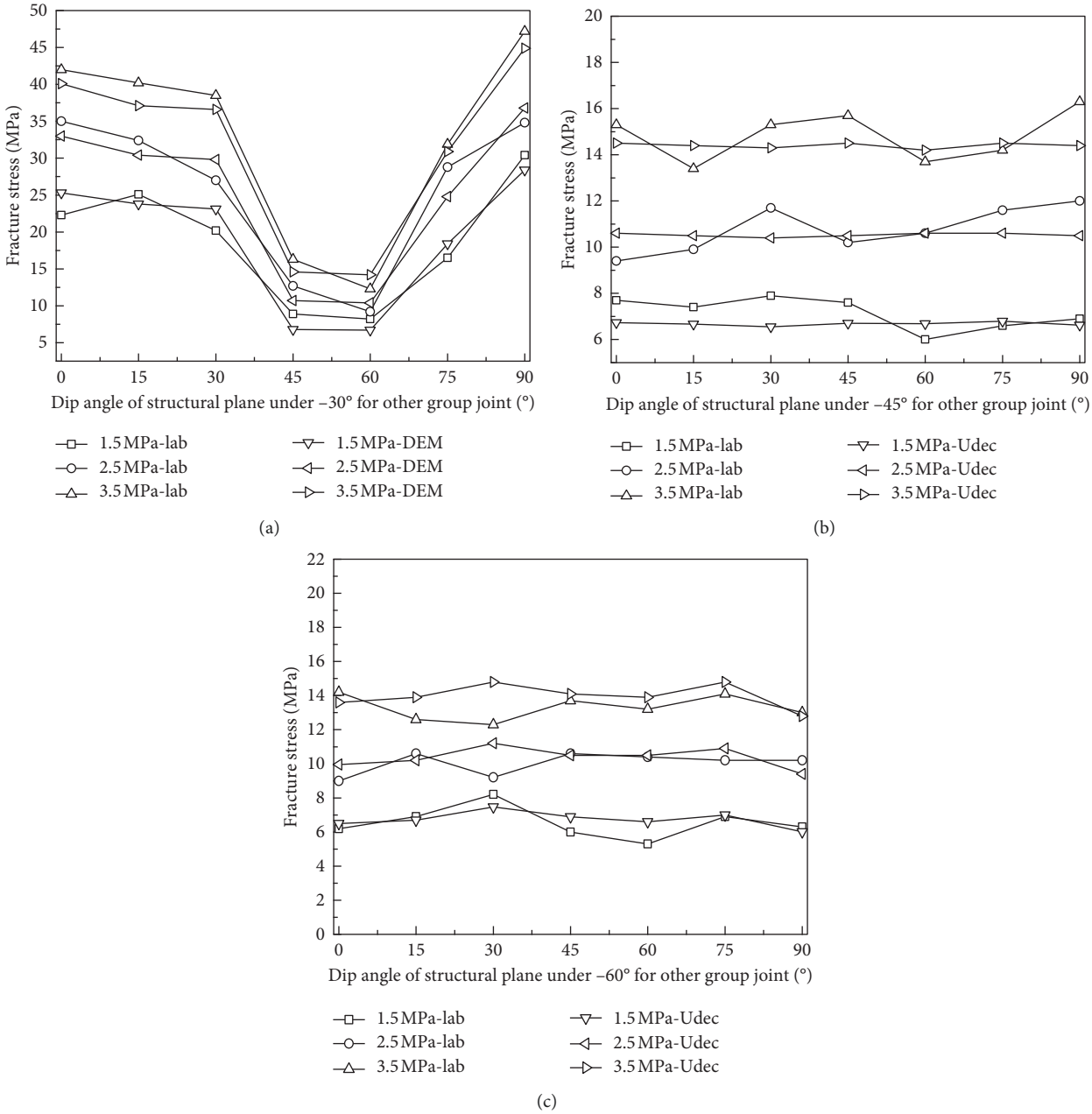

Figure 5: Comparison among numerically simulated and laboratory measured fracture stress value of rockmass with dip angles of (a) −30°, (b) −45°, and (c) −60° under different confining pressures (lab refers to laboratory value, and DEM refers to discrete element numerical simulation value).

stresses of rockmass with different spacing of structure planes under the confining pressure of 1.5 MPa is shown in Figure 9. The rockmass fracture stress values with the same confining pressure increases with the growing spacings of the structure planes. As shown, with the greater spacing, the influence of the spacing of the structure planes on rockmass strength becomes weaker. The density of the fracture stress under different spacings of structure plane may also reflect the influence of size on rockmass parameters, and the fracture stress values of rock samples with a size of 5 m is basically the lowest. The strength of rockmass increases with the increase in size, and the rockmass size effect presents in the numerical simulation. Generally, the fracture stress of the rock samples with a size of 5 m is little smaller than that of the rock samples with a size of 2 m. but if the rockmass size is larger than a critical value, the rockmass strength will keep stable with the increase of the rockmass size. This critical value is the representative elementary volume of rockmass, i.e., the REV of the rockmass.

The fracture stresses of rockmass with different spacing of structure plane under the confining pressure being 1.5 MPa with the numerical simulation method is shown in Figure 10. With the same confining pressure, the fracture stresses under different rockmass sizes change significantly,

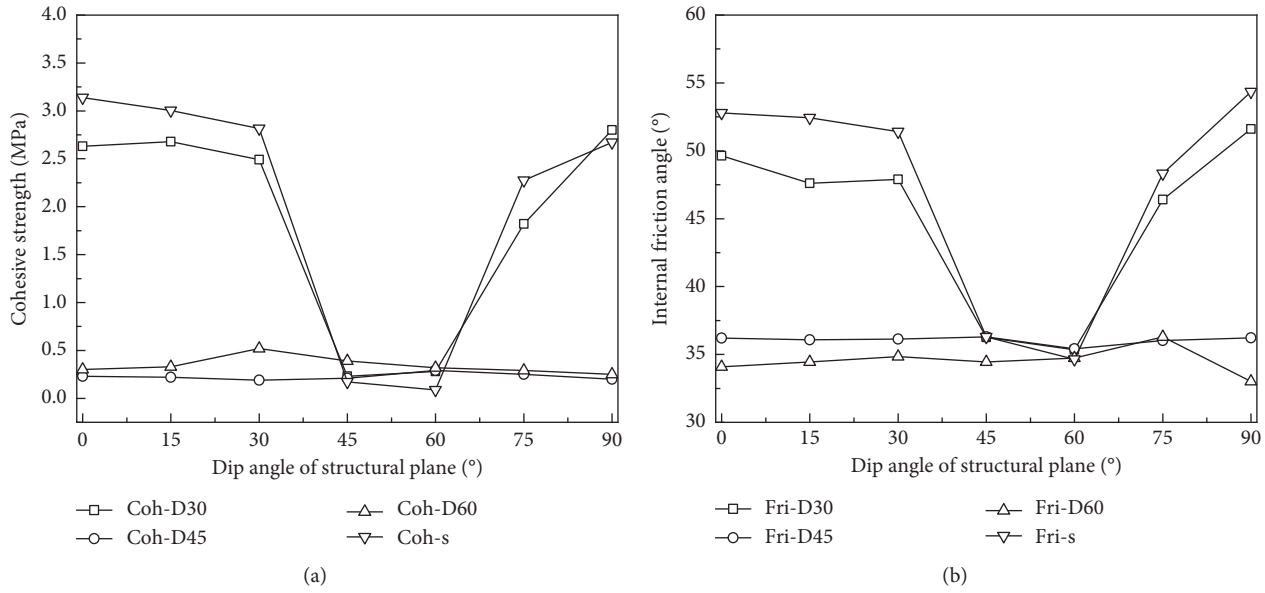

Figure 6: Graph showing numerically simulated values of (a) cohesive strength and (b) internal friction angle of rockmass with different dip angles.

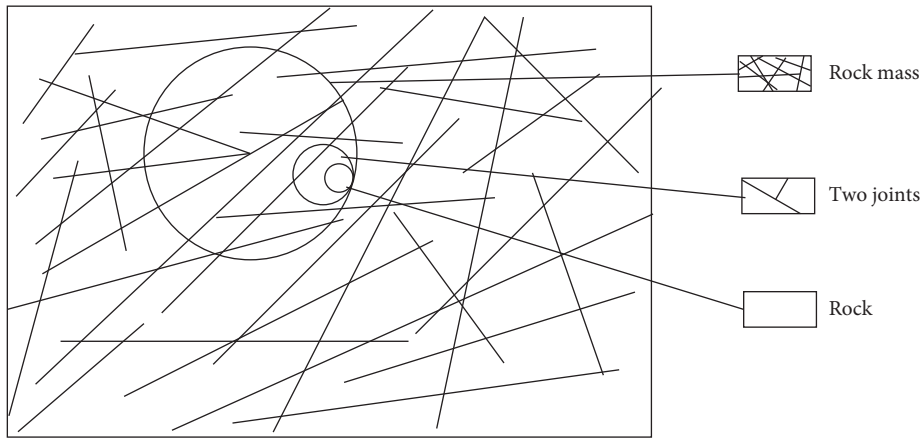

Figure 7: Size effects of rockmass.

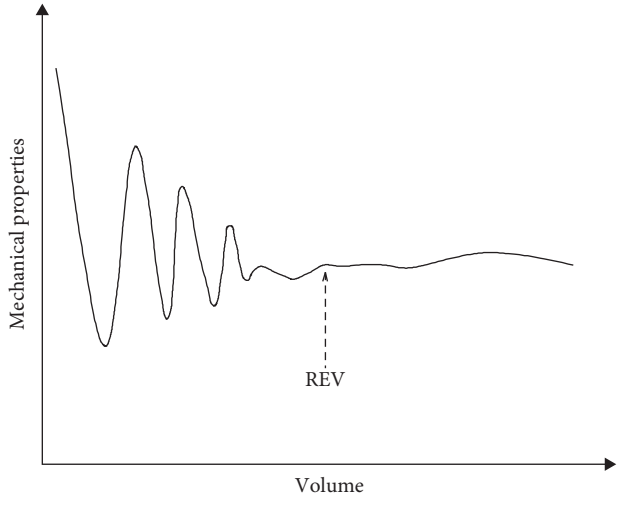

Figure 8: Representative elementary volume (REV).

especially between rock block and rockmass. As shown in Figures 10(a)–10(c), when the dip angle of rockmass with a single structure plane is 30°, 45°, and 60°, the rockmass strength changes greatly with rock sample size, and the fracture stress value of the rockmass is basically stable until the rockmass size greater than 5 m × 5 m. It can be seen from Figure 10(d), for the rockmass with double X-shaped structure planes, the fracture stress value is stable when the size reaches about 4 m × 4 m under the confining pressure of 1.5 MPa.

The REV of rockmass with double X-shaped structure planes is smaller than that of rockmass with a single structure plane, because the rockmass cut by a double structure plane is more fractured and uniform than that cut by a single structure plane. Therefore, from the perspective of probability, rockmass with double structure planes reach fracture earlier and more stably than those with a single structure plane. It also can be seen

Table 3: Fracture stresses of rockmass with different dip angles and spacing when the confining pressure is 1.5 MPa (a represents side length).

Geometry characteristics of structure plane		Fracture stress values under confining pressures 1.5 MPa/MPa							
Type	Dip angle (°)/space (m)	$H = 0.108$ m	$H = 0.108$ m	$a = 0.5$ m	$a = 1$ m	$a = 2$ m	$a = 3$ m	$a = 4$ m	$a = 5$ m	$a = 6$ m
Single joint	30/0.1	33.5 (no joint)	25.10	17.50	19.30	21.90	23.60	23.20	20.40	24.10
	45/0.1		9.99	3.30	2.50	2.62	3.10	1.68	2.61	2.87
	60/0.1		6.47	3.35	2.62	2.32	2.77	2.92	2.86	2.72
	30/0.3		25.10	20.60	18.70	20.90	22.30	20.80	21.00	22.80
	45/0.3		9.90	4.12	2.71	2.80	3.28	2.47	1.86	2.28
	60/0.3		6.50	6.47	4.20	3.05	3.12	2.71	2.46	3.42
	30/0.6		25.10	21.10	19.50	23.90	21.20	21.40	19.90	20.70
	45/0.6		9.97	3.70	3.16	4.21	4.27	2.43	2.12	2.31
	60/0.6		6.47	8.63	6.31	4.32	3.28	2.77	2.90	2.80
	30/1.0		25.10	21.10	20.10	20.50	23.10	20.40	19.70	22.00
	45/1.0		9.97	3.71	2.88	3.89	4.08	3.46	2.61	2.54
	60/1.0		6.57	8.64	7.62	4.67	4.74	2.98	3.05	2.87
X-shaped joint	30/0.1–45/0.1		9.16	4.15	4.12	3.95	3.38	3.57	3.78	3.79
	45/0.1–60/0.1		7.17	3.02	2.42	2.29	2.15	2.25	2.19	1.94
	60/0.1–30/0.1		7.34	2.87	2.71	2.27	2.29	2.27	2.32	2.35
	30/0.5–45/0.5		9.36	5.43	5.41	3.81	3.71	3.93	4.55	5.18
	45/0.5–60/0.5		7.16	3.78	2.61	3.15	2.96	2.53	2.54	2.31
	60/0.5–30/0.5		7.34	9.72	4.35	4.80	2.92	2.51	2.92	2.67
	30/1.0–45/1.0		9.35	6.20	5.20	4.90	4.31	4.38	4.41	4.58
	45/1.0–60/1.0		7.16	3.75	2.64	3.83	3.78	3.88	2.57	2.31
	60/1.0–30/1.0		6.99	9.72	9.30	5.70	5.00	3.55	3.56	2.80

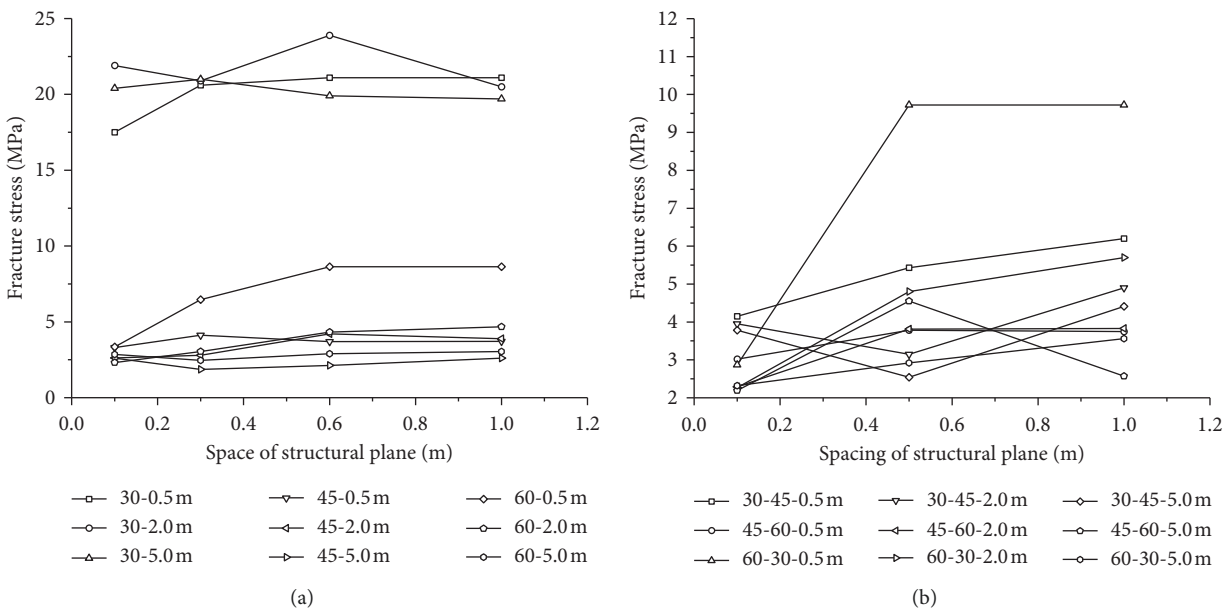

Figure 9: Fracture stresses of rockmass with different spacing of structure plane when the confining pressure is 1.5 MPa: (a) rockmass with a single structure plane and (b) rockmass with an X-shaped combined structure plane.

from Figures 9 and 10, the spacing of the structure plane and size effect have great influences on the rockmass mechanical parameters. When the spacing of the structure plane is not larger than 1 m and the size of the rock sample is larger than 4 m to 5 m, the rockmass mechanical parameters are basically stable. The REV values of rockmass with the geometric features of such a structure plane range from about 4 m × 4 m to 5 m × 5 m.

4. Conclusions

The triaxial numerical test was conducted by means of the discrete element method. The size effect of rockmass was studied by using the characteristics of the numerical test. The main conclusions are as follows:

(1) The dip angle has a significant effect on rockmass strength and stability. The rockmass fracture stress-dip

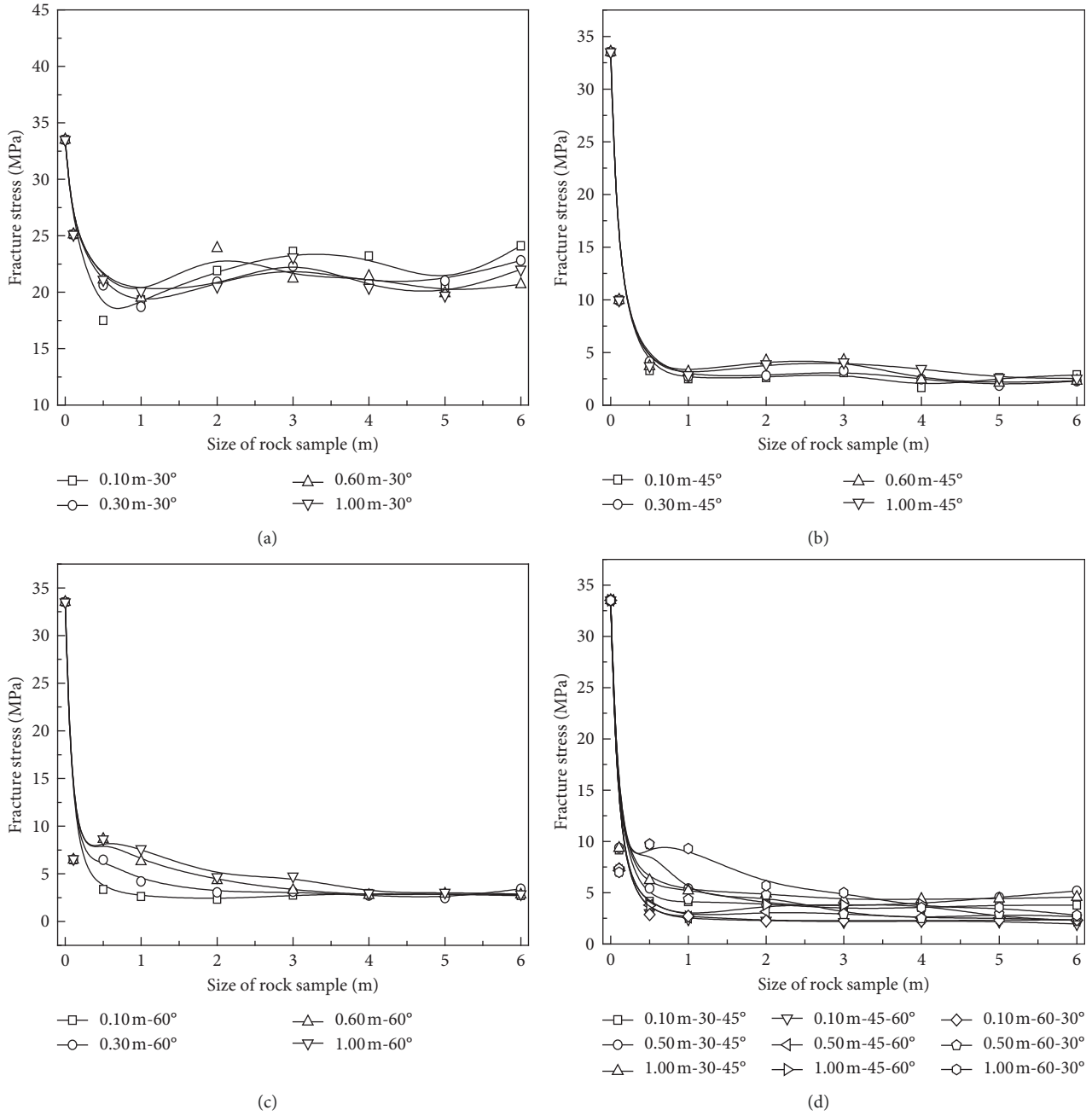

Figure 10: Numerical simulation results of fracture stress of rock samples with different spacings of structure planes under the confining pressure of 1.5 MPa: (a) dip angle of 30°; (b) dip angle of 45°; (c) dip angle of 60°, and (d) different sizes and different combined dip angles.

angle curve with a U-shaped distribution, and its minimum value for the dip angle being approximately $45^\circ + \varphi/2$ (approximately 60°). The strength of rockmass with the structure plane of horizontal ($\alpha = 0^\circ$) or vertical ($\alpha = 90^\circ$) is lager, and the shear fracture is dominant.

(2) The rockmass with X-shaped double structure plane has stronger strength than the one with the single structure plane. The fracture stress-dip angle curve of rockmass with slow dip angle combination has a U-shaped distribution. The rockmass with a steep dip angle combination are basically controlled by the adverse structure plane. The comprehensive rockmass mechanical parameters with a single structure plane are slightly higher than those with a double structure plane. The comprehensive cohesive strength and internal friction angle reduce gradually with a single-double structure plane.

(3) The spacing of the structure plane also has an impact on rockmass strength parameters. The strength of rockmass increases with the increase in spacing. The influence of size effect on rockmass mechanical

parameters is significant. With the increase in size, the mechanical parameters of rockmass decrease and then become stable. The representative elementary volume of rockmass on one project dam foundation is about 4 m × 4 m to 5 m × 5 m.

Data Availability

The data used to support the findings of this study are available from the corresponding author upon request.

Conflicts of Interest

The authors declare that they have no conflicts of interest.

Acknowledgments

This paper was financially supported by the National Natural Science Foundation of China (Grant nos. 41672258 and 41102162). The authors gratefully acknowledge Dr. Haotian Fan and Feng Zhu in Hohai University, China, for their help in numerical tests.

References

[1] M. Khamehchiyan, M. R. Dizadji, and M. Esmaeili, "Application of rock mass index (RMI) to the rock mass excavatability assessment in open face excavations," *Geomechanics and Geoengineering*, vol. 9, no. 1, pp. 63–71, 2014.

[2] H. Nourani, M. T. Moghadder, and M. Safari, "Classification and assessment of rock mass parameters in Choghart iron mine using P-wave velocity," *Journal of Rock Mechanics and Geotechnical Engineering*, vol. 9, no. 2, pp. 318–328, 2017.

[3] M. N. Bidgoli and L. Jing, "Anisotropy of strength and deformability of fractured rocks," *Journal of Rock Mechanics and Geotechnical Engineering*, vol. 6, no. 2, pp. 156–164, 2014.

[4] X. Fan, K. H. Li, H. P. Lai, Y. L. Xie, R. H. Cao, and J. Zheng, "Internal stress distribution and cracking around flaws and openings of rock block under uniaxial compression: a particle mechanics approach," *Computers and Geotechnics*, vol. 102, pp. 28–38, 2018.

[5] Y. Zhao, L Zhang, W. Wang, C. Pu, W. Wen, and J. Tang, "Cracking and stress–strain behavior of rock-like material containing two flaws under uniaxial compression," *Rock Mechanics and Rock Engineering*, vol. 49, no. 7, pp. 2665–2687, 2016.

[6] G. Z. Sun, *Rock Mass Structure Mechanics*, Science Press, Beijing, China, 1988.

[7] X. Wang, Y. Zhao, and X. Lin, "Determination of mechanical parameters for jointed rock masses," *Journal of Rock Mechanics and Geotechnical Engineering*, vol. 3, no. s1, pp. 398–406, 2011.

[8] Z. Y. Wang and P. J. Duan, "Determination of jointed mechanical parameters on the basis of triaxial compression test for rock mass," *Rock and Soil Mechanics*, vol. 32, no. 11, pp. 3219–3224, 2011.

[9] D. M. Lin, K. Y. Wang, and K. Li, "Modification of rock mass strength assessment methods and their application in geotechnical engineering," *Bulletin of Engineering Geology and the Environment*, vol. 76, no. 4, pp. 1471–1480, 2017.

[10] X. Q. He, C. S. Xu, K. Peng, and G. Huang, "Simultaneous identification of rock strength and fracture properties via scratch test," *Rock Mechanics and Rock Engineering*, vol. 50, no. 8, pp. 2227–2234, 2017.

[11] N. Bahrani and P. K. Kaiser, "Estimation of confined peak strength of crack-damaged rocks," *Rock Mechanics and Rock Engineering*, vol. 50, no. 2, pp. 309–326, 2017.

[12] Q. S. Liu, Y. C Tian, D. F. Liu, and Y. L. Jiang, "Updates to JRC-JCS model for estimating the peak shear strength of rock joints based on quantified surface description," *Engineering Geology*, vol. 228, no. 13, pp. 282–300, 2017.

[13] Y. J. Jiang, B. Li, and Y. Tanabashi, "Estimating the relation between surface roughness and mechanical properties of rock joints," *International Journal of Rock Mechanics and Mining Sciences*, vol. 43, no. 6, pp. 837–846, 2006.

[14] P. H. S. W. Kulatilake, J. Liang, and H. Gao, "Experimental and numerical simulations of jointed rock block strength under uniaxial loading," *ASCE Journal of Engineering Mechanics*, vol. 127, no. 12, pp. 1240–1247, 2001.

[15] Z. D. Cui, D. A. Liu, and F. Q. Wu, "Influence of dip directions on the main deformation region of layered rock around tunnels," *Bulletin of Engineering Geology and the Environment*, vol. 73, no. 2, pp. 441–450, 2014.

[16] Y. H. Xu and M. Cai, "Numerical study on the influence of cross-sectional shape on strength and deformation behaviors of rocks under uniaxial compression," *Computers and Geotechnics*, vol. 84, pp. 129–137, 2017.

[17] X. Fan, R. Chen, H. Lin, H. P. Lai, C. Y. Zhang, and Q. H. Zhao, "Cracking and failure in rock specimen containing combined flaw and hole under uniaxial compression," *Advances in Civil Engineering*, vol. 2018, Article ID 9818250, 15 pages, 2018.

[18] Y. Zhao, L. Zhang, W. Wang, J. Tang, H. Lin, and W. Wen, "Transient pulse test and morphological analysis of single rock fractures," *International Journal of Rock Mechanics and Mining Sciences*, vol. 91, pp. 139–154, 2017.

[19] L. Jing, "Block system construction for three-dimensional discrete element models of fractured rocks," *International Journal Rock Mechanics and Mining Sciences*, vol. 37, no. 4, pp. 645–659, 2000.

[20] J. P. Yang, W. Z. Chen, D. S. Yang, and J. Q. Yuan, "Numerical determination of strength and deformability of fractured rock mass by FEM modeling," *Computers and Geotechnics*, vol. 64, pp. 20–31, 2015.

[21] D. Huang, J. Wang, and S. Liu, "A comprehensive study on the smooth joint model in DEM simulation of jointed rock masses," *Granular Matter*, vol. 17, no. 6, pp. 775–791, 2015.

[22] X. Fan, K. H. Li, H. P. Lai, Q. H. Zhao, and Z. H. Sun, "Experimental and numerical study of the failure behavior of intermittent rock joints subjected to direct shear load," *Advances in Civil Engineering*, vol. 2018, Article ID 4294501, 19 pages, 2018.

[23] M. A. Oda, "Method for evaluating the representative elementary volume based on joint survey of rock mass," *Canadian Geotechnical Journal*, vol. 25, no. 3, pp. 281–287, 1988.

[24] T. Koyama, N. Fardin, L. Jing, and O. Stephansson, "Numerical simulation of shear induced flow anisotropy and scale dependent aperture and transmissivity evolutions of fracture replicas," *International Journal of Rock Mechanics and Mining Sciences*, vol. 43, no. 1, pp. 89–106, 2006.

[25] C. B. Zhou, Y. F. Chen, and Q. H. Jiang, "Representative elementary volume and mechanical parameters of fractured rock masses," *Journal of Geotechnical Engineering*, vol. 29, no. 8, pp. 1135–1142, 2007.

[26] P. T. Wang, T. H. Yang, T. Xu, M. F. Cai, and C. H. Li, "Numerical analysis on scale effect of elasticity, strength and

failure patterns of jointed rock masses," *Geosciences Journal*, vol. 20, no. 4, pp. 539–549, 2016.

[27] S. R. Sun, H. Y. Sun, Y. J. Wang, J. H. Wei, J. Liu, and D. P. Kanungo, "Effect of the combination characteristics of rock structure plane on the stability of a rock-mass slope," *Bulletin of Engineering Geology and the Environment*, vol. 73, no. 4, pp. 987–995, 2014.